CHEMMEDCHEM

CHEMISTRY ENABLING DRUG DISCOVERY

Accepted Article

Title: Cationic and Neutral N-Heterocyclic Carbene Gold(I) Complexes: Cytotoxicity, NCI-60 screening, Cellular Uptake, Inhibition of Mammalian Thioredoxin Reductase and ROS formation

Authors: Chen ZHANG, Catherine Hemmert, Heinz Gornitzka, Olivier CUVILLIER, Ming ZHANG, and Raymond Wai-Yin SUN

To be cited as: *ChemMedChem* 10.1002/cmdc.201800181

Link to VoR: http://dx.doi.org/10.1002/cmdc.201800181

A Journal of

ChemPubSoc Europe

WILEY-VCH

www.chemmedchem.org

WILEY-VCH

FULL PAPER

Cationic and Neutral *N*-Heterocyclic Carbene Gold(I) Complexes: Cytotoxicity, NCI-60 screening, Cellular Uptake, Inhibition of Mammalian Thioredoxin Reductase and ROS formation

Chen Zhang,[a] Catherine Hemmert,*[a] Heinz Gornitzka,*[a] Olivier Cuvillier,*[b] Ming Zhang,[c] and Raymond Wai-Yin Sun*[c]

[a] C. Zhang, Prof. Dr. H. Gornitzka, Dr. C Hemmert
LCC-CNRS, Université de Toulouse, CNRS, UPS, Toulouse, France.
E-mail: gornitzka@lcc-toulouse.fr, hemmert@lcc-toulouse.fr
[b] Dr. O. Cuvillier
Institut de Pharmacologie et de Biologie Structurale, Toulouse, Université de Toulouse, CNRS, UPS, Toulouse, France.
E-mail: olivier.cuvillier@inserm.fr
[c] M. Zhang, Prof. Dr. R. W.-Y. Sun
Department of Chemistry, The University of Hong Kong, Pokfulam, Hong Kong, P. R. China.
E-mail: rwysun@hku.hk

Supporting information for this article is given via a link at the end of the document.

Abstract: A structurally diverse library of fourteen gold(I) cationic bis(NHC) and neutral mono (NHC) complexes (whereas NHC = N-heterocyclic carbene) has been synthesized and characterized in this work. Four of them are new cationic gold(I) complexes containing functionalized NHCs with their X-ray structures presented. All of these complexes have been investigated for their anti-cancer activities in four cancer cell lines including a cisplatin-resistant variant and compared to a non-cancerous cell line. Among them, seven cationic gold(I) complexes were found to display high and specific cytotoxic activities towards cancer cells. Two of them were even capable to overcome cisplatin resistance. Two highly potent cationic complexes (**11** and **15**) were also submitted to the NCI-60 cancer panel for further cytotoxicity evaluation. Among the nine examined cancer subtypes, **15** showed a surprisingly high potency on leukemia, particularly towards CCRF-CEM with the GI_{50} value down to 79.4 nM. On the other hand, cationic complex **13** demonstrating a remarkable cytotoxicity against hepatocellular carcinoma was selected to get insights into its mechanistic aspects in HepG2 cells. Cellular uptake measurements were indicative of a good bioavailability. By various biochemical assays, this complex was found to effectively inhibit the thioredoxin reductase (TrxR) and its cytotoxicity towards the HepG2 cells was found to be ROS-dependent.

Introduction

A variety of gold-based complexes has long been identified to display promising pharmacological activities toward tuberculosis, arthritis and cancer.[1-3] To enhance the bioavailability as well as therapeutic efficacy, new generations of these complexes should be designed to have adequate aqueous stability under physiological conditions. In general, these complxes should also be hydrophilic enough to be soluble under physiologic conditions and lipophilic enough to pass membranes in order to reach their targets. One family of ligands, namely *N*-heterocyclic carbenes (NHCs), presents the features to design complexes combining all these characteristics. In these molecular entities gold has either oxidation state +1 or +3. In the field of anticancer gold(III) NHC complexes, important results have been presented by the groups of Che,[4-6] Gust,[7] Saha and Dinda.[8-10] Multiple anti-cancer targets for gold(III) have been identified by Che and coworkers, including topoisomerase I,[6] HSP60, vimentin, nucleophosmin, and YB-1.[4] It is well established that most NHC gold(III) complexes are not stable under biological conditions and are reduced by thiol-containing proteins to gold(I) species.[5] This could also explain very similar cytotoxic activities observed for gold(III) complexes and the corresponding gold(I) complexes. In the case of gold(I), neutral NHCAuX (X = Cl, Br, SR) complexes and cationic bisNHC gold(I) complexes have been investigated for their anticancer potency and in most cases the cationic complexes show higher cytotoxic activities than the neutral ones, probably due to the “labile” Au-Cl bond driving such complexes too sensitive toward thiol containing proteins.[11,12] The cytotoxic activities of the gold(I) complexes could be partially attributed to the specific binding of gold ions to sulfur and selenium containing biomolecules such as thioredoxin reductase (TrxR).[13-16] Neutral NHCAuCl complexes have been shown to be more active against isolated TrxR than cationic bisNHC gold(I) complexes.[11,12,17,18] Also this phenomenon can be explained by the stability of the complexes. More recently, alternative targets have been identified for gold(I) NHC complexes, as telomeric DNA G-quadruplex[19] and zinc finger proteins such as poly(ADP-ribose) polymerase 1 (PARP-1),[20] an enzyme involved in DNA repair and drug resistance mechanisms of cancer cells.

As an extension of our previous studies on bioactive NHC gold(I) complexes,[21-26] we prepared a family of nitrogen or sulfur containing NHC gold(I) complexes. In this context we herein present our studies on 14 NHC gold(I) complexes (four new and ten previously described ones[21,22,24,26]) covering five neutral and nine cationic NHC gold(I) complexes concerning their cytotoxic activities determined *in vitro* on four human cancer cell lines including one cisplatin resistant cell line and on one non-cancerous cell line to evaluate their selectivity. Two potent cationic gold(I) complexes have been selected and tested on a panel of 60 cell lines by the National Cancer Institute Developmental Therapeutic Screening. Moreover, cellular uptake, inhibition of isolated and intracellular thioredoxin reductase and ROS production have been studied for a bis(NHC) gold(I) complex.

Results and Discussion

Chemistry

The carbene precursors **2** and **3** (see Scheme 1) were synthesized as described in the literature.[21] In the case of proligands **1** and **4**, an excess of imidazole was heated under reflux with 1-(2-chloroethyl)piperidine hydrochloride and 3-chloro-*N*,*N*-dimethylpropylamine hydrochloride respectively, in aceronitrile. The most notable features in the ^{1}H and ^{13}C spectra of the imidazolium salts are the resonances for imidazolium protons (*H2*) located at 9.50-9.51 ppm and the corresponding imidazolium carbons (*C2*) in the range of 136.97-137.72 ppm. The resonance of the hydrochloride protons are comprised between 11.24 and 11.47 ppm. The High Resolution Mass Spectra (HRMS) of the proligands exhibit the classical peak correponding to [M – Cl –HCl] cations.

We have chosen the convenient transmetalation route to prepare the four gold(I) complexes **5**, **6**, **8**, and **10** (see Scheme 1). Firstly, the silver precursor complexes were prepared by deprotonation of the imidazolium salts **1-4**, with an excess of the mild base Ag_2O in dry methanol at room temperature. An ion exchange with one half equivalent of $AgNO_3$ dissolved in acetonitrile was performed, in order to avoid the formation of insoluble compounds or ionic species of type $[Ag(NHC)_2][AgCl_2]$. The carbene transfer reaction was thus carried out *in situ*, by adding one half equivalent of $Au(SMe_2)Cl$, with respect to the ligand. Gold(I) complexes **5**, **6**, **8**, and **10** were isolated as white or grey powders with yields ranging from 40 to 84%; all the synthesized complexes are highly stable towards air and moisture and soluble in CH_3CN, MeOH and DMSO.

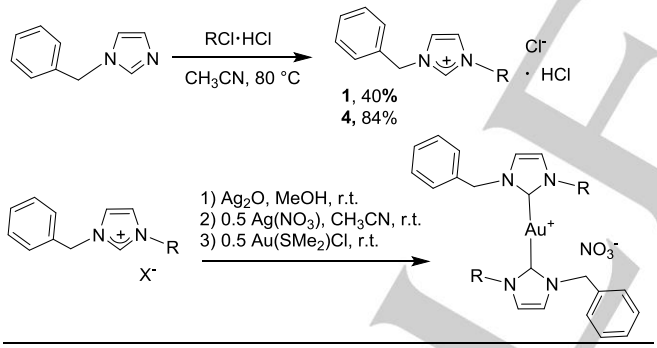

Ligand	R	X	Complex	Yield (%)
1	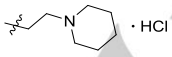	Cl	**5**	40
2[a]	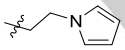	Br	**6**	50
3[a]	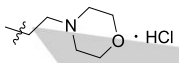	Cl	**8**	84
4	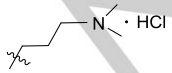	Cl	**10**	84

Scheme 1. Synthesis of gold(I) complexes **5-6, 8** and **10**. [a]Ref. 21.

NMR spectroscopy unequivocally demonstrates the formation of the gold(I) complexes with the absence of the proton resonance of the acidic imidazolium; the ^{13}C spectra show the resonance for the carbene carbon atoms at 183.96, 184.45, 183.95 and 183.84 ppm, for **5**, **6**, **8**, and **10**, respectively. The elemental analysis of the gold(I) complexes correspond to the general $[AuL_2][NO_3]$ formula for **5-8** and the HRMS exhibit the classical peak corresponding to the cationic fragment $[M – NO_3^-]^+$ for **5-8**.

Crystals of **5** and **8** have been obtained by slow gas-phase diffusion of diethyl ether into the concentrated solutions of the complexes in acetonitrile. Crystals of **6** and **10** suitable for X-ray diffraction analysis were obtained by slow evaporation from methanol solutions of these complexes.

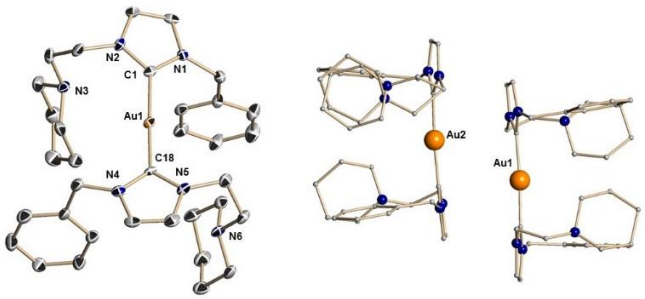

Figure 1. Molecular structure of **5** in the solid state. The cationic part is depicted on the left side at a 30% level thermal ellipsoid plot. For clarity only one of two independent cations is shown and H-atoms, non-coordinating anions and a disorder of one piperidine group are omitted. The arrangement of the two independent cations is shown on the right side. Selected bond distances [Å] and angles [°]: Au1-C1 2.020(9), Au1-C18 1.995(9), C1-Au1-C18 176.5(4).

The cations of **5** formed a kind of dimers in the solid state (see Figure 1) with a distance Au1-Au2 of 4.023 Å which is too long to be considered as an aurophilic interaction. This arrangement explains the fact that the four side-arms of the two NHC ligands are placed on the same side in report to the NHC-Au-NHC plane. The NHC planes in each cation show only slight torsions of 7° and 9°, respectively. The gold atoms are coordinated in a classical nearly linear manner for gold(I). The benzyl groups are in trans position related to the C-Au-C line.

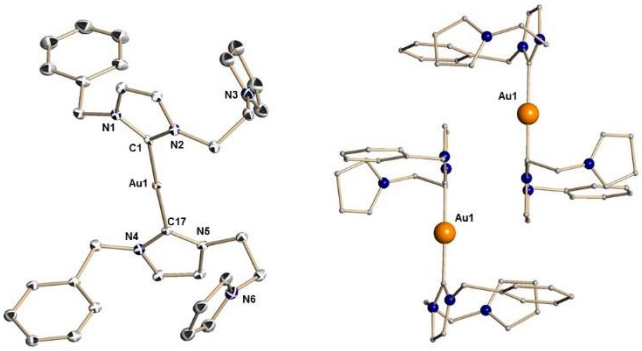

Figure 2. Molecular structure of **6** in the solid state. The cationic part is depicted on the left side at a 30% level thermal ellipsoid plot. For clarity H-atoms and non-coordinating anions are omitted. The arrangement of the cations in the solid state is shown on the right side. Selected bond distances [Å] and angles [°]: Au1-C1 2.035(9), Au1-C17 2.034(9), C1-Au1-C17 178.1(4).

The cations of **6** formed also a kind of dimers in the solid state (see Figure 2) with a distance Au1-Au1 of 5.764 Å which is also too long to be considered as an aurophilic interaction. In this arrangement the two side arms of one NHC ligand are on the same side of the connected NHC plane, but in this case the side arms of the other NHC of the cation are on the other side of the NHC-Au-NHC plane. In **6** the NHC planes show a rotation of about 20° around the C-Au-C axis. The gold atoms are again coordinated in a classical nearly linear manner for gold(I). Figure 3 shows that the anions are located in canals between chains of cations.

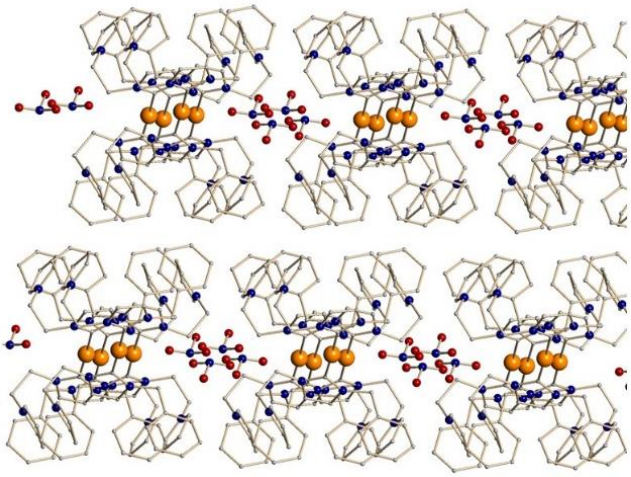

Figure 3: Packing of **6** in the solid state.

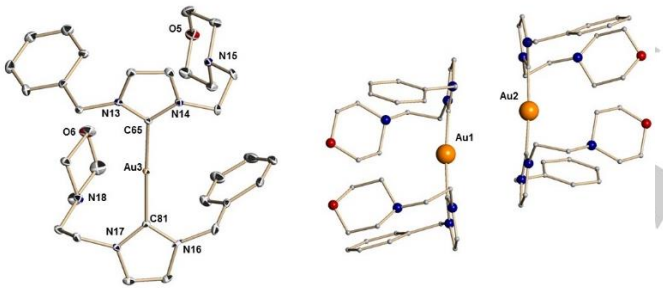

Figure 4: Molecular structure of **8** in the solid state. The cationic part is depicted on the left side at a 50% level thermal ellipsoid plot. For clarity only one of four independent cations is shown, H-atoms, non-coordinating anions and a disorder of one morpholine group are omitted. The arrangement of the cations in the solid state is shown on the right side. Selected bond distances [Å] and angles [°]: Au3-C65 2.014(7), Au3-C81 2.015(7), C65-Au3-C81 174.8(3).

Complex **8** crystalized in the monoclinic space group *P2₁* with four independent molecules in the asymmetric unit. The absolute structure parameter refined to x = 0.245(7) and a disorder present in only one morpholine group has been treated. As in cations **5** and **6**, cations of **8** formed a kind of dimers in the solid state (see Figure 4) with gold-gold distances out of range for aurophilic interactions (Au1-Au2 4.136 Å and Au3-Au4 4.228 Å). All four independent cations show the same structural main features. As observed in **5**, the four side-arms of the two NHC ligands of one cation are placed on the same side in report to the NHC-Au-NHC plane. The NHC planes in each cation show only slight torsions between 10° and 15°. The gold atoms are coordinated in a classical nearly linear manner for gold(I). The benzyl groups are in trans position related to the C-Au-C line. In **8** the anions are more like located in wholes as in canals (see Figure 5).

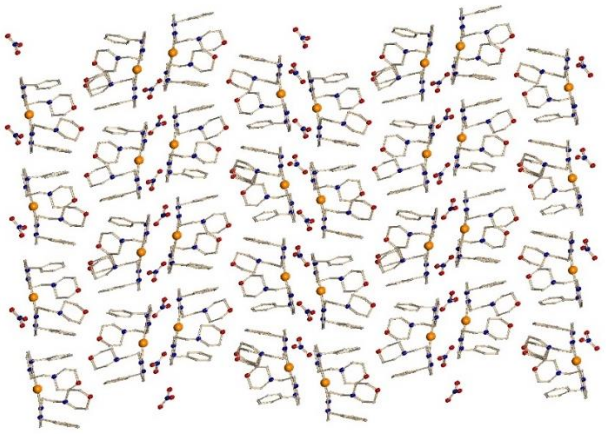

Figure 5: Crystal packing of **8**.

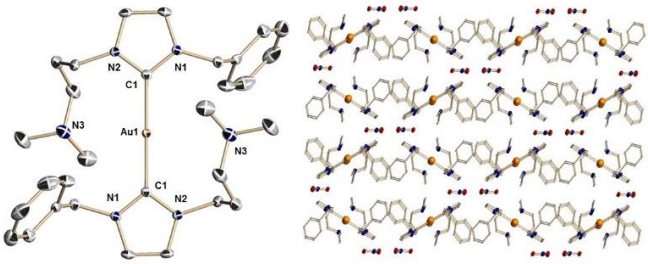

Figure 6: Molecular structure of **10** in the solid state. The cationic part is depicted on the left side at a 50% level thermal ellipsoid plot. For clarity H-atoms and non-coordinating anions are omitted. The crystal packing is shown on the right side. Selected bond distances [Å] and angles [°]: Au1-C1 2.012(2), C1-Au1-C1 180.0.

In **10** only half a molecule is present in asymmetric unit with the gold atom located on an inversion center (see Figure 6). Cations are isolated from each other and the anions are placed in canals. The shortest gold-gold distances are 7.53 Å. The two NHC planes are perfectly coplanar. The side arms of one NHC ligand are placed on the same side of the plane of the corresponding NHC ring. The side arms of the second NHC ligand of one cation are situated on the other side of the NHC-Au-NHC plane. Looking on this plane the benzyl substituents are in trans position to each other.

Antiproliferative activity

The *in vitro* anticancer activities of fourteen gold(I) carbene complexes **5**–**18** toward four human cancer cell lines, including ovarian carcinoma (A2780 and its cisplatin-resistant variant A2780cis), hepatocellular carcinoma (HepG2 and HepAD38) and the non-cancerous Madin–Darby canine kidney epithelial (MDCK) cell line, were examined by MTT assay [MTT = 3-(4,5-dimethylthiazol-2-yl)-2,5-diphenyltetrazolium bromide] and

compared to the reference drug cisplatin.[27] The cytotoxicity at 72 h towards these cells was depicted in terms of IC_{50} values and summarized in Table 1.

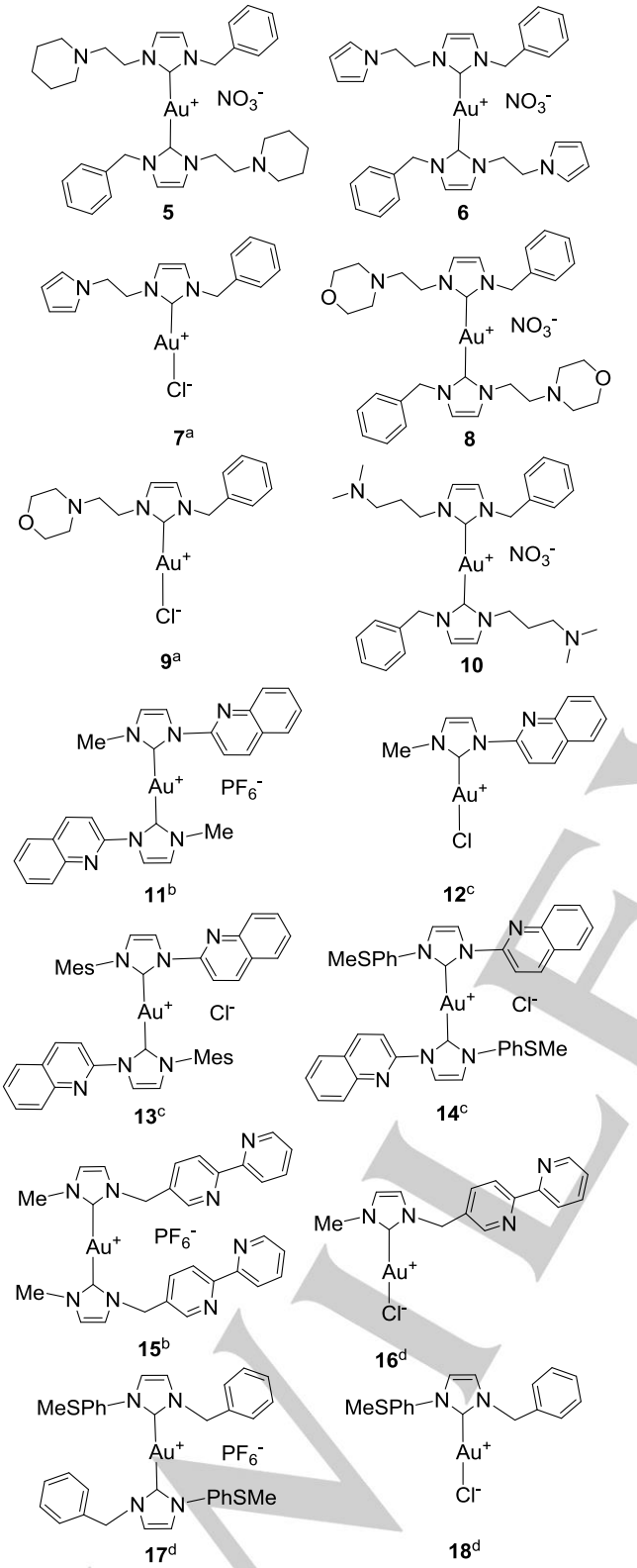

Scheme 2. Gold(I) complexes tested in this study. [a]Ref. 21, [b]Ref. 26, [c]Ref. 24 and [d]Ref. 22.

The cationic gold(I) bis(NHC) complexes **5**, **6**, **11**, **13**, **14**, **15** and **17** were found to exhibit potent anticancer activities towards the cancer cell lines, with IC_{50} values spanning over the range from 0.11 to 5 μM, with the exception of 16 μM obtained for **11** on HepG2. The mean feature of five (**6**, **11**, **13**-**15**) of the seven active complexes is the presence of an aromatic amine, namely, pyrrole, quinoline and bipyridine, the two other ones containing a piperidine for **5** and a thioanisole for **17**. The most effective complexes resulted to be **13** and **15** with IC_{50} values from 0.11 to 0.78 μM, followed by **6** and **17** (IC_{50} = 0.17-3.1 μM) on the four tested cancerous cell lines. These results are indicative of a bioactivity of the complexes for the cancer cells dependent on the nature of the groups on the NHC ligands. Importantly, this series of cationic gold(I) complexes showed much higher cytotoxicity against ovarian carcinoma (IC_{50} from 0.11 to 3.2 μM) cell lines than against hepatocellular carcinoma ones (IC_{50} from 0.46 to 5.0 μM, if we exclude the remote value of 16 μM obtained for **11** towards HepG2). However, it should be mentioned that the commercial drug Sorafenib currently used to treat hepatocarcinoma displays a high IC_{50} value of 6.4 μM on the HepG2 cell line.[28] Notably, the gold complexes **13** and **14** were more cytotoxic toward the resistant ovarian cell line A2780cis, with resistant ratios IC_{50}(A2780cis)/IC_{50}(A2780) of 0.16 and 0.31, respectively, indicating that these three complexes are able to overcome the resistance to cisplatin which has a resistant ratio of around 10. All the cationic bis(NHC) gold(I) complexes were found to display a lower cytotoxicity towards the normal MDCK cells as compared to the cancer cells.

Among the tested family of cationic gold(I) bisNHC complexes only the two complexes **8** and **10** containing a morpholine entity and an aliphatic amine, respectively, showed no activity against the cancer cell lines. Concerning the five neutral NHC-Au-Cl complexes, four of them (**7**, **9**, **16** and **18**) displayed low or no activity towards all the tested cell lines with IC_{50} values ranging from 9 to over 50 μM, the best value being obtained for complex **18** bearing a thioanisole group, towards the ovarian carcinoma cell line A2780. In contrast, the neutral complex **12** involving a quinoline moiety showed IC_{50} values below 10 μM and was highly cytotoxic towards the cisplatin-resistant ovarian carcinoma cells (A2780cis) with an IC_{50} value of 2.9 μM, when compared to the reference molecule cisplatin. The cytotoxicity of **12** towards a non-cancerous origin derived cell line MDCK was also examined and the IC_{50} value was found to be 23 μM. In comparison to the A2780cis cell line, **12** displayed a 7.9-fold higher selectivity towards cancerous cells than normal cells.

From this screening, the mono(NHC) chloro-substituted complexes appear in general less effective than their bis(NHC) counterparts due to the strength of the Au-NHC bonds compared to the labile chloride group, thus making the chloride derivatives more reactive and prone to be deactivated by different cellular components. The complexes may also be inactive because of their low solubility in water or because they are not taken up by the tumor cells. Nevertheless, we prepared the stock solutions of all our complexes in DMSO in which they are totally soluble and no precipitation was observed after dilution in physiological medium.

Moreover, this general trend can be related to an effect commonly known for delocalized lipophilic cations (DLCs).[29,30] Due to the electric gradient between membranes' inner and outer layers, DLCs can penetrate the hydrophobic barrier of the cellular membranes and accumulate selectively in mitochondria of tumor cells, due to a difference of around 60 mV between the mitochondrial membrane potentials of cancerous and healthy cells.

NCI-60 screening

The antiproliferative activity of two of the highest selective cytotoxic complexes, namely **11** and **15** involving quinoline and methylbipyridine functionalized groups, respectively, was further evaluated *in vitro* by the National Cancer Institute Developmental Therapeutic Program (NCI DTP) with a panel of 60 human cancer cell lines being part of nine cancer subtypes. First, a single dose of NCI-60 (10 μM) was assayed, giving average growth percentages of 14.18 for **11** and 35.91 for **15**, which indicates sufficient cytotoxicity to warrant NCI-60 screening at five doses spanning the concentration range 10^{-8}-10^{-4} molar. The growth inhibition patterns were analyzed using graphs representing the mean response over all the 60 cell lines and schematized by plotting positive and negative values along a vertical line. Three endpoints were determined: GI_{50} (concentration for 50% inhibition of growth), TGI (concentration for 100% inhibition of growth) and LC_{50} (concentration decreasing by 50% the original cell number) (see Supporting Information). The midpoints of the GI_{50} mean graphs were -5.47 and -5.57 corresponding to GI_{50} mean values of 3.36 and 2.69 μM for **11** and **15**, respectively. A general trend demonstrated a relatively similar profile for the two cationic gold(I) complexes that showed greater potency on leukemia, colon and breast cancer cell lines compared to the other cancer cell subtypes. Figure 7 illustrates the average GI_{50} values for **11** and **15** from the five-dose screen against the nine subtypes of cancer cells tested. Complex **15** displayed higher activity with GI_{50} values ranging from 0.541 to 7.50 μM than **11** (GI_{50} values from 2.07 to 6.68 μM). Notably, **15** showed particularly high cytotoxic activities toward cancer cell lines of CCRF-CEM (79.4 nM, leukemia), K-562 (501 nM, leukemia) and SR (398 nM, leukemia), NCI-522 (100 nM, lung), COLO-205 (398 nM, colon), OVCAR-4 (794 nM, ovarian), MCF7 (316 nM, breast) and MDA-MB-468 (316 nM, breast) cells.

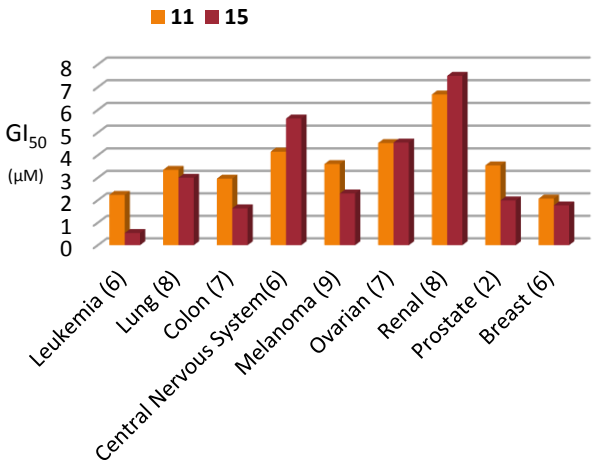

Figure 7. Average GI_{50} values (μM) for complexes **11** and **15** from the NCI-60 Five-Dose Screen. In brackets, the number of cancer cell lines tested for each subtype.

These values were compared to clinically relevant anticancer drugs with known MAOs (Figure 8), using GI_{50} mean graphs from the NCI (log(high concentration) = -4.0). Oxaliplatin is a third-generation organoplatinum agent, used in combination with other antineoplastic drugs in the treatment of gastrointestinal tract cancer, colorectal liver metastasis, ovarian cancer and non-small cell lung cancer.[31] Like cisplatin, oxaliplatin acts as an alkylating agent on DNA, forming platinated intrastrand cross-links between two adjacent guanine bases d(GpG) or two adjacent guanine–adenine bases d(GpA), which constitute the major cytotoxic lesions. Paclitaxel (Taxol®), isolated from *Taxus brevifolia* and discovered in the early 1960's through a plant screening program initiated by the NCI and playing a crucial role in the treatment of ovarian, breast and non-small cell lung cancer[32,33], exhibited a broad spectrum of anti-cancer activity as illustrated in Figure 8. Paclitaxel has a unique mechanism of action that disrupts the micro-tubule dynamics, thus inducing mitotic arrest that leads to cell death.[34] Irinotecan, a camptothecin derivative, is a key anticancer drug for the treatment of metastatic colorectal cancer and acts as a DNA topoisomerase 1 poison.[35] The chemotherapeutic agent 5-fluorouracil commonly used to treat colorectal cancer inhibits thymidylate synthase and also induce p53-dependent cell cycle arrest and apoptosis in response to DNA damage.[36] Finally, imatinib mesylate, a tyrosine kinase inhibitor, is the most frequently used as first-line therapy for chronic myeloid leukemia.[37] Collectively, the data depicted in Figure 6 highlight a high anticancer activity of **15**, in all cases better than that of the platinum containing drugs cisplatin and oxaliplatin. Taxol is more cytotoxic than **15** against nearly all cell lines presented in Figure 8 except ovarian cancer cell line OVCAR-4. Concerning the more specific drugs irinotecan, fluorouracil and imatinib, **15** is nearly more active towards the selected cancerous cell lines. Irinotecan and fluorouracil show very good activities against Leukemia SR, moreover, fluorouracil is active against MCF7 and as expected against the colon cancer cell line COLO 205. Imatinib shows only a very specific cytotoxicity against K-562, a chronic myeloid leukemia cell line.

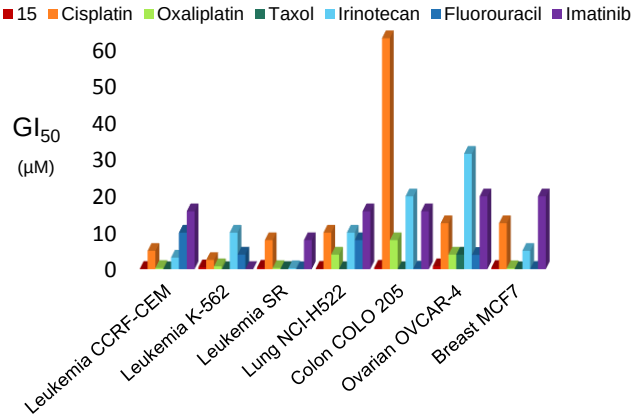

Figure 8. Selected GI_{50} values (μM) for complex **15** and clinically anticancer drugs from the NCI-60 Five-Dose Screen.

In order to understand the difference between **15** and oxaliplatin, we compared the normalized dose-response profiles at five concentration levels from 10^{-4} to 10^{-8} molar of both complexes on leukemia CCRF-CEM and NSC lung cancer cell line NCI-522 (see Figure 9).

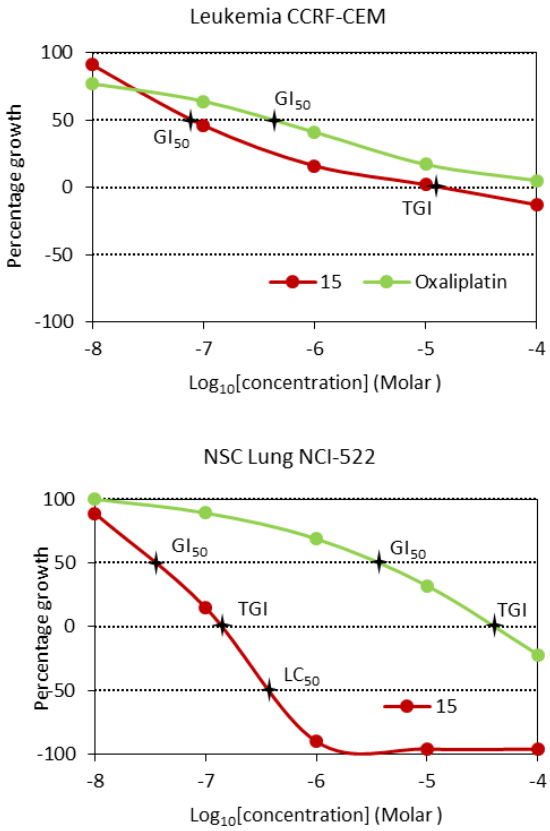

Figure 9. Dose Response curves of **15** and oxaliplatin for two relevant cancer cell lines from the NCI-60 Five-Dose Screen.

Concerning CCRF-CEM cell line, the antiproliferative activity of both complexes were relatively close to each other with GI_{50} values in the nanomolar range, 83.4 nM and 316 nM for **15** and oxaliplatin, respectively. The TGI value of 13.4 µM for **15** was in the concentration range of measurement, which was not the case for LC_{50} of **15** and TGI and LC_{50} of oxaliplatin (> 100 µM). The situation was significantly different concerning NCI-522 cell line. While the GI_{50} (33.8 nM), TGI (139 nM) and LC_{50} (407 nM) values of **15** reflected a strong dual cytostatic/cytotoxic activity, oxaliplatin was more than 100 times less active on this cell line with GI_{50} = 3.98 µM, TGI = 31.6 µM and LC_{50} > 100 µM.

Cellular uptake

The cationic bis(NHC) gold complex **13**, containing a bulky mesityl group and a quinoline moiety, was the most lipophilic complex of the studied series and showed high cytotoxic potency and selectivity. It belongs to the DLCs class and is expected to easily penetrate the cell membrane and selectively accumulate in the mitochondria of the cancer cells. Accordingly, complex **13** was chosen for further investigations regarding its mechanism of action.

Hepatocellular carcinoma is one of the most common cancers worldwide and is highly resistant to available chemotherapeutic agents, administered either alone or in combination.[38] Complex **13** showed the higher cytotoxicity towards the HepG2 cell line compared to the other tested gold(I) complexes. Therefore, we evaluated the cellular uptake of complex **13** in HepG2 cells by a method based on gold quantification, by inductively coupled plasma atomic emission spectroscopy (ICP-AES). The measurements were performed under serum-free cell culture medium in order to avoid competition with proteins binding. For this purpose, the cells were incubated with a 2.0 µM solution of complex **13** for 1, 2 and 4 h at 37 °C and 5% CO_2, and the gold and protein levels of the cells were determined by ICP-AES and the Bradford method, respectively. Complex **13** showed a cellular gold level of 0.68 ± 0.25 µg per mg of cell protein after 1 h of exposure, which then increased over the total incubation period of 4 h to 3.04 ± 0.43 µg per mg of cell protein. This indicates a fast cellular uptake of **13**, in good agreement with antiproliferative activity.

Inhibition of mammalian TrxR

The ubiquitous selenoenzyme TrxR is considered as one of the most relevant targets for gold complexes, as gold displays a high affinity to selenol groups.[1,13,39-42] TrxR is a NADPH-dependent flavoprotein responsible for cell homeostasis regulation and inhibition of TrxR could lead to apoptosis through a mitochondrial pathway.[43,44] At the molecular level, a selenocysteine residue in the *C*-terminal active site of TrxR is considered as the ultimate target for gold species, and covalent binding with gold(I) ions has been suggested.[45] A variety of gold complexes including auranofin have been shown to be potent inhibitors of TrxR. The potential of complex **13** to inhibit the target enzyme TrxR was studied *in vitro* on purified rat liver TrxR. Moreover, inhibition of reducing agents present in cell extracts has been tested *in vitro*. Both tests used a previously reported assay based on the NADPH dependent reduction of the sulfide bond of the substrate 5,5'-dithiobis-2-nitrobenzoic acid (DTNB) by the isolate enzyme.[46] Complex **13** was able to inhibit isolated TrxR in the low micromolar range with an IC_{50} value of 2.1 µM. In order to evaluate the inhibition of cellular reducing agents, HepG2 cells were exposed to complex **13** in graded concentrations for 1 h and after treatment, the cells were monitored colorimetrically for their ability to reduce DTNB. The IC_{50} value for cellular reducing agents was 2.0 µM, which is very close to the isolated TrxR one. This potent inhibition of TrxR is comparable to recently reported cationic gold(I) complexes containing ferrocenylated bis(NHC), which are able to reduce the cellular TrxR activity in the range of 55 to 60% in A549 lung cancer cells treated with 2.5 µM of complexes.[47] Lately, another series of cationic C-4 substituted biscarbene gold(I) complexes with high cytotoxic activities in several cancer cells was found to display moderate to low efficacy (IC_{50} from 16.3 to 127.8 µM) towards the targeted isolated mammalian TrxR enzyme.[11] From literature data, neutral mono(NHC) gold(I) complexes are in general more effective TrxR inhibitors than their cationic bis(NHC) analogs. This is well illustrated by independent studies showing that in the case of bis[1,3-diethyl-4,5-diarylimidazolylidene] ligands, Au(I) bis(NHC) complexes are weakly or not active with IC_{50} between 3.4 and >10 µM whereas Au(I) NHC-Br complexes show values ranging from 0.812 to 4.37 µM;[18] the same trend is observed for gold(I) complexes with benzimidazolylidene ligands with EC_{50} of 0.36 and 4.89 µM for the neutral and the cationic complexes, respectively.[12] The neutral complexes are less stable in solution and in particular in physiological medium because of the lability of the halide, which generates a vacant site on the gold and allows

a fast coordination with selenocysteine residue of the TrxR. Overall, as discussed in the introduction section, the TrxR appears to be a common relevant target among others shared for this kind of gold complexes.

Effects on intracellular ROS levels

Generation of reactive oxygen species (ROS) is a key characteristic of apoptotic cell death. ROS are mostly the products of the physiological mitochondrial cell metabolism and are involved in cellular redox homeostasis. Their formation may perturb the cellular antioxidant defense system. Au(I)-NHC complexes have been reported to generate ROS, which may be due to the inhibition of the TrxR, one of the antioxidant enzymes present in the mammalian cell together with catalase, glutathione peroxidase and superoxide dismutase that carry out the removal of ROS from the cell.[8,9,12,48-52]

In order to examine whether ROS played a role in complex **13** cytotoxicity, we used *N*-acetylcysteine (NAC), a ROS scavenger, to study its effect on cell viability. For this purpose, HepG2 cells were pretreated with NAC at different concentrations (2 mM, 5 mM and 10 mM) for 1 h before the gold(I) complex was added. After treatment, the results showed that NAC substantially dose-dependently reduced both ROS accumulation and cytotoxicity of complex **13** in HepG2 cells (see Figure 10). These data suggest that cytotoxicity induced by the Au(I)bis(NHC) complex is ROS-dependent. This effect is in line with other previously reported gold complexes, yet we have to be careful when comparing different experimental protocols. Two examples of intracellular ROS levels determined using the NAC scavenger are illustrated hereafter. Au(I)-NHC complexes derived from cyclophanes, which displayed higher anti-cancer activity and selectivity than cisplatin against four cancer cell lines (Hela, A549, MDA-MB-231) including the cisplatin-resistant cell line A549R, were selectively localized in the mitochondria. Mechanistic studies showed that both complexes have no effect on cell cycle and induced apoptosis in cancer cells through caspase- and ROS-dependent pathways.[49] Furthermore, a gold(I) bis(NHC) complex bearing amide side arms markedly inhibited the growth of HCT116, HepG2 and A549 cancerous cells and displayed anti-melanoma activity *in vitro* and *in vivo* towards the highly metastatic mouse melanoma B16F10 cell line. It induced ROS formation and p53-dependent apoptosis in B16F10 cells involving the mitochondrial death pathway and suppressed melanoma tumor growth by regulating the level of pro- and anti-apoptotic factors.[50]

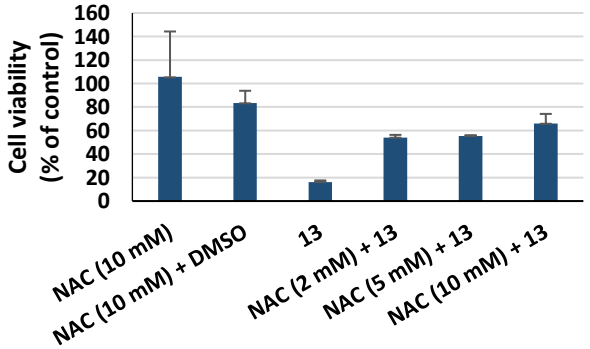

Figure 10. Effects of different concentrations of NAC on **13**-induced cytotoxicity.

Conclusions

Four cationic gold(I) bis(NHC) complexes containing nitrogen functionalized ligands have been synthetized and fully characterized. A panel of fourteen neutral and cationic gold(I) NHC(s) complexes was first tested for *in vitro* anticancer potency towards four cancerous cell lines including a cisplatin resistant one. Although the neutral complexes were for most part not effective, seven cationic complexes displayed high antiproliferative activity and the best relevant ones include an aromatic amine on the NHC scaffold. Two of the most potent complexes were further screened for cytotoxicity by the NCI at a five dose concentration on 60 cancerous cell lines involving nine cancer subtypes and one exhibited major *in vitro* activity on leukemia, colon and breast cancer cells. Further mechanism studies on one lead-complex showed by monitoring the cellular uptake that this kind of complexes are biologically stable. Moreover, this complex was an inhibitor of TrxR, a common target for various gold(I) complexes and its cytotoxicity was ROS-dependent.

Experimental Section

Materials

All complexation reactions were performed under an inert atmosphere of dry nitrogen by using standard vacuum line and Schlenk tube techniques. 1-(Benzyl)-3-[2-(1*H*-pyrrol-1-yl)ethyl]-1*H*-imidazol-3-ium bromide (**2**), 1-(benzyl)-3-[2-(morpholine-4-yl)ethyl]-1*H*-imidazol-3-ium chloride hydrochloride (**3**) and complexes **7** and **9**,[21] complexes **11** and **15**,[26] complexes **12**-**14**[24] and complexes **16-18**[22] were prepared according literature procedure. All other reagents were used as received from commercial suppliers. Reactions involving silver compounds were performed with the exclusion of light. Cell Proliferation Kit I (MTT) was purchased from Alfa Aesar. Human ovarian carcinoma cell lines A2780 and its cisplatin-resistant variant A2780cis were purchased from Sigma-Aldrich Chemical Co. Human hepatocellular carcinoma (HepG2) were obtained from American Type Culture Collection (ATCC). HepAD38 is a stably transfected hepatoblastoma cell line, which secretes HBV-like particles and expresses high levels of HBV DNA into its surrounding medium (supernatant) and was sincerely given by Prof. K. K. Lau (The University of Hong Kong). A normal Madin-Darby canine kidney epithelial cells (MDCK) cell line was obtained commercially from ATCC. Cell-culture flasks, 96-well plates and Transwell® 24-well plates were purchased from Nalge Nunc. Culture medium, other medium constituents, and phosphate-buffered saline (PBS) were from Gibco BRL.

Instrumentation

^{1}H (300 or 400 MHz) and ^{13}C NMR spectra (75 or 101 MHz) were recorded at 298 K on Bruker AV300 or Bruker AV400 spectrometers in DMSO-d_6, CD_3CN and CD_3OD as solvents. Elemental analyses were carried out by the "Service de Microanalyse du Laboratoire de Chimie de Coordination (Toulouse)". HRMS were performed with a Thermo Finnigan MAT 95 XL spectrometer using electrospray ionization (ESI) by the "Service de Spectrométrie de Masse de Chimie UPS-CNRS" (Toulouse). The absorbance for MTT assay was measured using a Promega E7031 microplate reader. ICP-AES analysis were performed with a Thermo Scientific iCAP 6300 DUO spectrometer by the "Service Analyses du Laboratoire de Chimie de Coordination (Toulouse)".

Synthesis of proligands 1 and 4 and complexes 5-6, 8 and 10

The following picture describes the numbering of H (^{1}H NMR) and C (^{13}C NMR). These notations are used in the following experimental section.

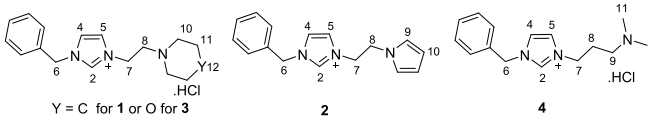

1-(Benzyl)-3-[2-(piperidine-4-yl)ethyl]-1*H*-imidazol-3-ium chloride hydrochloride (1)

In a pressure flask, 1-(2-chloroethyl)piperidine hydrochloride (290 mg, 1.58 mmol) and benzylimidazole (300 mg, 1.9 mmol) were dissolved in 10 mL of dry acetonitrile. The mixture was stirred at 80 °C for 48 h. After cooling to room temperature, the precipitate formed was filtered, washed with diethyl ether and dried under vacuum to give a white solid (370 mg, 60% yield). Anal. Calcd. For $C_{17}H_{25}Cl_2N_3$: C, 59.65; H, 7.36; N, 12.28. Found: C, 59.44; H, 7.58; N, 12.18. ^{1}H NMR (300 MHz, DMSO-d_6): δ 11.47 (s, 1H, HCl), 9.50 (s, 1H, H2), 7.92 (s, 1H, H5), 7.82 (s, 1H, H4), 7.49-7.39 (m, 5H, benzyl), 5.44 (s, 2H, H6), 4.73 (t, 2H, *J*= 6 Hz, H7), 3.62-3.40 (m, 4H, H10), 2.97-2.87 (m, 2H, H8), 1.92-1.67 (m, 6H, H11, H12). ^{13}C NMR (75 MHz, DMSO-d_6): δ 137.72 (1C, C2), 135.02 (1C, benzyl), 129.41 (2C, benzyl), 129.22 (1C, benzyl), 128.94 (2C, benzyl), 123.29 (1C, C5), 123.17 (1C, C4), 54.61 (1C, C6), 52.78 (2C, C10), 52.52 (1C, C7), 43.54 (1C, C8), 22.43 (2C, C11), 21.66 (1C, C12). HRMS (ES$^+$): calcd. for $C_{17}H_{24}N_3$ 270.1970; found 270.1975.

1-[2-Dimethyl)propyl]-benzylimidazolium chloride hydrochloride (4)

In a pressure flask, 3-chloro-*N*,*N*-dimethylpropylamine hydrochloride (300 mg, 1.90 mmol) was suspended in 10 mL of dry acetonitrile. After the solid was completely dissolved, benzylimidazole (450 mg, 2.85 mmol) was slowly added to the solution. The reaction mixture was stirred for 72 h at 80 °C. After cooling to room temperature, the solvent was removed under vacuum to give a pale yellow paste. The paste was dissolved in a small amount of acetonitrile and precipitated with diethyl ether. The precipitate was filtered, washed with diethyl ether and dried under vacuum to give a pale yellow solid (200 mg, 33% yield). Anal. Calcd. For $C_{15}H_{23}N_3Cl_2$: C, 56.97; H, 7.33; N, 13.29. Found: C, 57.09; H, 7.38; N, 13.31.^{1}H NMR (400 MHz, DMSO-d_6): δ 11.24 (s, 1H, HCl), 9.51 (s, 1H, H2), 7.90 (s, 1H, H5), 7.86 (s, 1H, H4), 7.46-7.40 (m, 5H, benzyl), 5.46 (s, 2H, H6), 4.35 (t, 2H, *J*= 7.2 Hz, H7), 3.06 (t, 2H, *J*= 7.2 Hz, H9), 2.73 (s, 6H, H11), 2.32-2.25 (m, 2H, H8). ^{13}C NMR (100 MHz, DMSO-d_6): δ 136.97 (1C, C2), 135.22 (1C, benzyl), 129.45 (2C, benzyl), 129.21 (1C, benzyl), 128.81 (2C, benzyl), 123.28 (1C, C5), 123.08 (1C, C4), 53.42 (1C, C6), 52.43 (1C, C7), 46.73 (1C, C9), 42.37 (2C, C11), 24.74 (1C, C8). HRMS (ES$^+$): calcd. for $C_{15}H_{22}N_3$ 244.1814; found 244.1823.

Complex 5

In a Schlenk tube 1-benzyl-3-(2-(piperidin-1-yl)ethyl)-1*H*-imidazol-3-ium chloride hydrochloride (100 mg, 0.29 mmol) was suspended in 10 mL of dry methanol and Ag_2O (69 mg, 0.29 mmol) was added. The mixture was stirred at room temperature for 3 h under nitrogen in the dark. A solution of $AgNO_3$ (25 mg, 0.15 mmol) in 2 mL of acetonitrile was added and the mixture was stirred for 1 h. Finally, Au(SMe$_2$)Cl (43 mg, 0.15 mmol) was added and after stirring for 1 h, the mixture was filtered through a pad of celite. The solvent was evaporated under reduced pressure to give a white solid (40 mg, 40% yield). Anal. Calcd. For $C_{34}H_{46}AuN_7O_3$: C, 51.19; H, 5.81; N, 12.29. Found: C, 51.29; H, 5.63; N, 12.31.^{1}H NMR (400 MHz, CD_3CN): δ 7.35-7.23 (m, 14H, benzyl, H4, H5), 5.36 (s, 4H, H6), 4.23 (t, 4H, *J*= 6 Hz, H7), 2.67 (t, 4H, *J*= 6 Hz, H8), 2.36 (t, 8H, *J*= 4.8 Hz, H10), 1.47-1.39(m, 12H, H11, H12).^{13}C NMR (100 MHz, CD_3CN): δ 183.96 (2C, C2), 136.89 (2C, C2), 128.85 (4C, benzyl), 128.19 (2C, benzyl), 127.12 (4C, benzyl), 122.62 (2C, C5), 121.80 (2C, C4), 58.84 (2C, C6), 54.36 (4C, C10), 54.02 (2C, C7), 48.68 (2C, C8), 25.88(4C, C11), 23.98 (2C, C12). HRMS (ES+): calcd. for $C_{34}H_{46}AuN_6$ 735.3449; found 735.3448.

Complex 6

In a Schlenk tube 3-(2-(1*H*-pyrrol-1-yl)ethyl)-1-benzyl-1*H*-imidazol-3-ium bromide (100 mg, 0.3 mmol) was suspended in 10 mL of dry methanol and Ag_2O (67.3 mg, 0.3 mmol) was added. The mixture was stirred at room temperature for 3 h under nitrogen in the dark. A solution of $AgNO_3$ (25 mg, 0.15 mmol) in 2 mL of acetonitrile was added and the resulting mixture was stirred at room temperature overnight. Then the mixture was filtered through a pad of celite. After that, Au(SMe$_2$)Cl (44 mg, 0.15 mmol) was added and after stirring for 1 h, the mixture was filtered through a pad of celite. The solvent was evaporated under reduced pressure to give a grey solid (50 mg, 50 % yield). Anal. Calcd. For $C_{32}H_{34}AuN_7O_3$: C, 50.46; H, 4.50; N, 12.87. Found: C, 50.22; H, 4.60; N, 12.80. ^{1}H NMR (300 MHz, CD_3CN): δ 7.37-7.04 (m, 14H, benzyl, H4, H5), 6.39 (t, 4H, *J*= 2.1 Hz, H10), 5.97 (t, 4H, *J*= 2.1 Hz, H11), 5.24 (s, 4H, H6), 4.42 (t, 4H, *J*= 6 Hz, H7), 4.24 (t, 4H, *J*= 6 Hz, H8). ^{13}C NMR (75 MHz, CD_3CN): δ 184.45 (2C, C2), 136.61 (2C, benzyl), 128.79 (4C, benzyl), 128.15 (2C, benzyl), 127.18 (4C, benzyl), 122.35 (2C, C5), 121.79 (2C, C4), 120.66 (4C, C10), 108.49 (4C, C11), 53.94 (2C, C6), 52.30 (2C, C7), 49.40 (2C, C8). HRMS (ES$^+$): calcd. for $C_{32}H_{34}AuN_6$ 699.2510; found 699.2509.

Complex 8

In a Schlenk tube 1-benzyl-3-(2-morpholinoethyl)-1*H*-imidazol-3-ium chloride hydrochloride (100 mg, 0.29 mmol) was suspended in 10 mL of dry methanol and Ag_2O (67.3 mg, 0.29 mmol) was added. The mixture was stirred at room temperature for 3 h under nitrogen in the dark. A solution of $AgNO_3$ (25 mg, 0.15 mmol) in 2 mL of acetonitrile was added and the mixture was stirred for 1 h. Finally, Au(SMe$_2$)Cl (43 mg, 0.15 mmol) was added and after stirring for 1 h, the mixture was filtered through a pad of celite. The solvent was evaporated under reduced pressure to give a grey solid (97 mg, 84% yield). Anal. Calcd. For $C_{32}H_{42}AuN_7O_5$: C, 47.94; H, 5.28; N, 12.23. Found: C, 48.08; H, 5.35; N, 12.29. ^{1}H NMR (300 MHz, CD_3CN): δ 7.37-7.22 (m, 14H, benzyl, H4, H5), 5.36 (s, 4H, H6), 4.23 (t, 4H, *J*= 6 Hz, H7), 3.52 (t, 8H, *J*= 4.8 Hz, H10), 2.72 (t, 4H, *J*= 6 Hz, H8), 2.39(t, 8H, *J*= 4.8 Hz, H9). ^{13}C NMR (75 MHz, CD_3CN): δ 183.95 (2C, C2), 136.87 (2C, benzyl), 128.89 (4C, benzyl), 128.24 (2C, benzyl), 127.10 (4C, benzyl), 122.61 (2C, C5), 121.92 (2C, C4), 66.49 (4C, C11), 58.42 (2C, C6), 54.05 (2C, C7), 53.44 (4C, C10), 48.24 (2C, C8). HRMS (ES$^+$): calcd. for $C_{32}H_{42}AuN_6O_2$ 739.3035; found 739.3036.

Complex 10

In a Schlenk tube 1-benzyl-3-(3-(dimethylamino)propyl)-1*H*-imidazol-3-ium chloride hydrochloride (146 mg, 0.46 mmol) was suspended in 10 mL of dry methanol and Ag_2O (106 mg, 0.46 mmol) was added. The mixture was stirred at room temperature for 3 h under nitrogen in the dark. A solution of $AgNO_3$ (39 mg, 0.23 mmol) in 2 mL of acetonitrile was added and the mixture was stirred for 1 h. Finally, Au(SMe$_2$)Cl (67 mg, 0.23 mmol) was added and after stirring for 1 h, the mixture was filtered through a pad of celite. The solvent was evaporated under reduced pressure to give a grey solid (143 mg, 84% yield). Anal. Calcd. For $C_{30}H_{42}AuN_7O_3$: C, 48.32; H, 5.68; N, 13.15. Found: C, 48.25; H, 5.71; N, 13.28. ^{1}H NMR (400 MHz, CD_3OD): δ 7.45-7.24 (m, 14H, benzyl, H4, H5), 5.41 (s, 4H, H6), 4.27 (t, 4H, *J*= 6.8 Hz, H7), 2.30 (t, 4H, *J*= 6.8 Hz, H9), 2.21 (s, 12H, H10), 2.08-2.01 (m, 4H, H8). ^{13}C NMR (100 MHz, CD_3OD): δ 183.84 (2C, C2), 136.67 (2C, benzyl), 128.66 (4C, benzyl), 128.03 (2C, benzyl), 126.89 (4C, benzyl), 122.22 (2C, C5), 121.95 (2C, C4), 55.63 (2C, C6), 53.97 (2C, C7), 48.78 (2C, C9), 44.01 (4C, C11), 28.65 (2C, C8). HRMS (ES$^+$): calcd. for $C_{30}H_{42}AuN_6$ 683.3136 found 683.3130.

Crystallographic data for 5, 6, 8 and 10

All data were collected at low temperature (100(2) K) using oil-coated shock-cooled crystals on a Bruker-AXS APEX II diffractometer with MoKα radiation (λ = 0.71073 Å). The structures were solved by direct methods[53] and all non hydrogen atoms were refined anisotropically using the least-squares method on F^2.[54] The absolute structure of **8** has been refined.[55]
5: $C_{34}H_{46.5}AuN_7O_{3.5}$, Mr = 806.25, crystal size = 0.40 x 0.10 x 0.02 mm^3, triclinic, space group $P\bar{1}$, a = 10.684(2) Å, b = 16.145(2) Å, c = 21.292(2) Å, α = 79.396(3)°, β = 77.511(3)°, γ = 77.607(3)°, V = 3465.6(7) Å^3, Z = 4, 48878 reflections collected, 9811 unique reflections (R_{int} = 0.0526), R1 = 0.0538, wR2 = 0.1089 [I>2σ(I)], R1 = 0.0674, wR2 = 0.1140 (all data), residual electron density = 2.641 e Å^{-3}.
6: $C_{32}H_{34}AuN_7O_3$, Mr = 761.63, crystal size = 0.20 x 0.10 x 0.05 mm^3, triclinic, space group $P\bar{1}$, a = 10.835(1) Å, b = 11.485(1) Å, c = 12.716(1) Å, α = 76.585(4)°, β = 77.134(4)°, γ = 84.412(4)°, V = 1498.7(2) Å^3, Z = 2,

48878 reflections collected, 9811 unique reflections (R_{int} = 0.0526), R1 = 0.0491, wR2 = 0.1271 [I>2σ(I)], R1 = 0.0586, wR2 = 0.1338 (all data), residual electron density = 2.345 e Å^{-3}.
8: $C_{32}H_{42}AuN_7O_5$, Mr = 801.69, crystal size = 0.30 x 0.30 x 0.20 mm^3, monoclinic, space group *P2$_1$*, *a* = 10.984(1) Å, *b* = 30.847(3) Å, *c* = 19.590(2) Å, *β* = 90.277(2)°, V = 6637.4(9) Å^3, Z = 8, 110310 reflections collected, 56863 unique reflections (R_{int} = 0.0363), R1 = 0.0538, wR2 = 0.1220 [I>2σ(I)], R1 = 0.0630, wR2 = 0.1265 (all data), absolute structure factor x = 0.245(7), residual electron density = 6.675 e Å^{-3}.
10: $C_{30}H_{42}AuN_7O_3$, Mr = 745.67, crystal size = 0.30 x 0.20 x 0.20 mm^3, monoclinic, space group *C2/c*, *a* = 17.575(1) Å, *b* = 21.290(1) Å, *c* = 9.851(1) Å, *β* = 121.108(2)°, V = 3155.7(2) Å^3, Z = 4, 31004 reflections collected, 4798 unique reflections (R_{int} = 0.0480), R1 = 0.0173, wR2 = 0.0359 [I>2σ(I)], R1 = 0.0338, wR2 = 0.0402 (all data), residual electron density = 0.692 e Å^{-3}.
CCDC 1819420-1819423 contain the supplementary crystallographic data. These data can be obtained free of charge from The Cambridge Crystallographic Data Centre via www.ccdc.cam.ac.uk/data_request/cif.

Cell culture and growth inhibitory assay (MTT assay)
The cell lines were maintained in cell culture media (Eagle's minimum essential medium for MDCK; Dulbecco's Modified Eagle's Medium for HepG2 and HepAD38, RPMI-1640 medium for A2780 and A2780cis) supplemented with 10% fetal bovine serum, 100 U/mL penicillin, and 100 µg/mL streptomycin at 37 °C humidified atmosphere with 5% CO_2. Cell growth inhibitory effects of all the complexes were determined by MTT assay.[27] Briefly, cells were seeded in 96-well plates and incubated for overnight prior to be examined. All of the complexes were dissolved in DMSO. The concentration of the complexes was calculated according to the elemental composition of the complexes determined by the elemental analyses. Media in the presence of the tested complexes were added and serially diluted to various concentrations (from 40 µM to 0.3 µM). The maximum concentration of DMSO in media did not exceed 0.5 % (v/v). The cells were incubated for 72 h and followed by the addition of MTT solution. After 1 h, the formed formazan was dissolved by adding dimethyl sulfoxide (DMSO) and the absorbance of the solution at 560 nm was measured by using a microtitre plate reader. The IC_{50} values of the complexes (the concentrations of drug that is required for 50 % growth inhibition) were determined from the plots of the cell viability percentage *versus* the complex concentration. For each set of data, at least three independent experiments have been conducted.

NCI-60 Screening
Complexes **11** and **15** were first accepted by the National Cancer institute (Bethesda, MD) for single-dose screens at a concentration of 10^{-5} M against a panel of 60 human cancer cell lines, allowing growth percentages for each tested cell line. The two complexes were then tested twice for a five-dose NCI-60 screen spanning the concentration range of 10^{-8}-10^{-4} M, giving rise to GI_{50}, TGI and LC_{50} values of **11** and **15** for the 60 cell lines. The protocols used by the NCI are available on the NCI's Developmental Therapeutics Program web site.[56] GI_{50}, TGI and LC_{50} values of **15** were compared to those of publicly available NCI-60 DTP data (concentration range of 10^{-8}-10^{-4} M) for six clinically used anticancer drugs.

Cellular uptake studies
The cellular metal uptake was determined as described according to a previously described method.[12] Briefly, for the cellular uptake into HepG-2 human liver cancer cells, the cells were cultured until at least 80% confluence in 75 cm^2 flasks. Stock solution of complex **13** in sterile DMSO was prepared and diluted with cell culture medium to a final concentration of 2 µM (freshly prepared, final DMSO concentration of 0.1 % v/v). The cell culture medium was replaced by the fresh medium containing the gold complexes, and the flasks were incubated at 37 °C and 5% CO_2 for 1 and 4 h. After the desired incubation period, the cellular uptake was stopped by removing the cell culture medium. The cells were washed with PBS (10 mL), and then the pellets were collected after 10 min of trypsinization (0.05% trypsin-EDTA solution (10 mL) and centrifugation (room temperature, 1500 rpm, 5 min). Cells were resuspended in Mili-Q water (1 mL) and lysed by sonication for 30 s. The protein contents of lysates were determined by the Bradford method. 100 µL of samples were digested in 300 µL of 70 % HNO_3 at 70 °C for 2 h and room temperature overnight, then diluted 1:100 in ultrapure water for inductively coupled plasma atomic emission spectroscopy (ICP-AES) analysis. Results were calculated from the data obtained from three independent experiments and are expressed as microgram of gold per milligram of protein.

Inhibition of mammalian TrxR
To determine the inhibition of mammalian TrxR, an established microplate-reader-based assay was performed with minor modifications.[39] For this propose, commercially available rat liver TrxR (from Sigma-Aldrich) was used and diluted with distilled water to achieve 3.5 U/mL. Complex **13** was freshly dissolved as stock solution in sterile DMSO. 25 µL aliquot of the enzyme and either 25 µL potassium phosphate buffer (pH 7.0) containing complex **13** in graded concentrations or 25 µL buffer without the complex but DMSO (positive control) were added. The resulting solution (final DMSO concentration of 0.5 % v/v) was incubated at 37 °C for 75 min with moderate shaking in a 96-well plate. To each well, 225 µL of the reaction mixture (1.0 mL reaction mixture consists of 500 µL 100 mM potassium phosphate buffer pH 7.0, 80 µL 100 mM EDTA solution pH 7.5, 20 µL 0.2 % BSA, 100 µL of a 20 mM NADPH and 300 µL distilled water) was added and the reaction was initiated immediately by adding 25 µL of 20 mM DTNB solution. After thorough mixing, the formation of TNB was monitored by a microplate reader at 405 nm at 1 min intervals for 10 measurements. The increase of TNB concentration over time followed a linear tendency ($r^2 \geq 0.99$), and the enzymatic activities were calculated as the slopes (increase in absorbance per second) thereof. Non-interference with the assay components was confirmed by a negative control experiment using an enzyme-free test compound. IC_{50} values were calculated as the concentration of the complex decreasing the enzymatic activity of the untreated control by 50%.

Cellular activity of reducing agents present in the cell
The cellular activity of reducing agents present in the cell was determined according a previously described method.[5] Cells were counted and seeded at 2x10^5 per well in 6-well plates and incubated for 24 h. Complex **13** was freshly dissolved as stock solution in sterile DMSO, and the stock solution was diluted with cell culture medium to graded concentrations (final DMSO concentration of 1 % v/v). The cell culture medium was replaced by fresh medium containing gold complexes, and the plates were incubated for 1 h at 37 °C and 5% CO_2. Afterwards, the cells were washed with PBS for three times, and 100 µL of cold lysis buffer (50 mM phosphate buffer, pH 7.4, 1 mM EDTA, 0.1 % Triton-X 100) were added to the plates. Cell lysis was carried out on ice for 5 min and the cell lysates were collected and stored at -80 °C. The protein contents of lysates were determined by the Bradford method. Then cell lysates (10 µg) were added to 100 µL of reaction buffer (50 mM phosphate buffer, pH 7.4, 1 mM EDTA and 0.2 mM NADPH). Finally, 5,5'-dithiobis (2-nitrobenzoic acid) (DTNB, final concentration of 3 mM) was added to initiate the reaction and the cellular TrxR activity was determined as increases in O.D. 410 nM in 10 min. All the results were calculated from data obtained in three independent experiments.

Measurement of intracellular reactive oxygen species (ROS)
For *N*-acetyl-cysteine (NAC) treatment, the cells were pre-treated with different concentrations of NAC (2, 5 and 10 mM) for 1 h, then gold complex **13** was added for an additional 72 h. After incubation, cells were incubated at 37 °C and 5% CO_2 with 25 µL MTT solution (5 mg/mL; Sigma-Aldrich) in 24-well plates for approximately 3 h. The cytotoxicity was determined as described above.

Acknowledgements

This work was supported by the Centre National de la Recherche Scientifique (CNRS) and CZ thanks the Chinese Scholarship

Council (CSC) for a PhD grant. RWYS acknowledge the funding support by Guangdong Natural Science Foundation Project (2016A030313064). The authors greatly acknowledge the National Cancer Institute at Bethesda/Maryland/USA.

Keywords: gold · *N*-heterocyclic carbene · anti-cancer · NCI-60 screening · thioredoxin reductase

Table 1. Cytotoxic activity of gold(I) NHC complexes expressed as IC_{50} (μM) values towards selected cancer and normal cell lines as determined by MTT assay (72 h).

Complex	A2780cis	A2780	HepG2	HepAD38	MDCK
5	2.8±0.6	2.1±0.4	4.8±1.5	4.5±1.7	10±3
6	0.97±0.11	0.91±0.23	3.1±1.1	1.1±0.2	5.9±1.5
7	23±6	38±11	>50	>50	>50
8	44±11	28±9	>50	>50	>50
9	>50	>50	>50	>50	>50
10	20±3	11±2	>50	>50	>50
11	1.2±0.2	0.81±0.2	16±4	3.2±0.8	>20±8
12	2.9±0.5	8.5±1.7	8.5±1.6	9.6±2.0	23±5
13	0.11±0.02	0.67±0.3	0.46±0.12	0.39±0.13	3.0±0.5
14	1.0±0.2	3.2 ±0.8	5.0±0.9	1.7±0.3	9.6±1.8
15	0.74±0.18	0.12±0.02	0.48±0.13	0.78±0.14	2.8±0.6
16	>50	>50	>50	>50	>50
17	0.36±0.1	0.17±0.04	0.97±0.14	1.3±0.2	2.1±0.6
18	19±3	9.0±1.8	23±6	14±2	20±3
Cisplatin	34±2.4	3.2±0.61	4.31±1.10	12±1.3	27±3.8

The IC_{50} values represent the concentrations of the complexes and compounds causing 50% inhibition of cellular growth. Data are expressed as mean ± standard error μM and are resulted from at least three independent experiments.

References:

[1] I. Ott, *Coord. Chem. Rev.* **2009**, *253*, 1670-1681.
[2] C. M. Che and R. W. Y. Sun, *Coord. Chem. Rev.* **2009**, *253*, 1682-1691.
[3] F. Shaw III, *Chem. Rev.* **1999**, 99, 2589.
[4] T. Zou , B. Cao, P. Y. Lee, Y. M. E. Fung, D. Hu, C. N. Lok, C. M. Che, *Angew. Chem. Int. Ed.* **2017**, *56*, 3892-3896.
[5] T. Zou, C. T. Lum, S. S. Y. Chui, C. M. Che, *Angew. Chem. Int. Ed.* **2013**, *52*, 2930-2933.
[6] J. J. Yan, A. L. F. Chow, C. H. Leung, R. W. Y. Sun, D. L. Ma, C. M. Che, *Chem. Commun.* **2010**, *46*, 3893-3895.
[7] W. Liu, K. Bensdorf, M. Proetto, U. Abram, A. Hagenbach, R. Gust, *J. Med. Chem.* **2011**, *54*, 8605-8615.
[8] B. K. Rana, A. Nandy, V. Bertolasi, C. W. Bielawski, K. D. Saha, J. Dinda, *Organometallics* **2014**, *33*, 2544-2548.
[9] J. Dinda, A. Nandy, B. K. Rana, V. Bertolasi, K. D. Saha, C. W. Bielawski, *RSC Adv.* **2014**, *4*, 60776-60784.
[10] T. Samanta, R. N. Munda, G. Roymahapatra, A. Nandy, K. D. Saha, S. S. Al-Deyab, J. Dinda, *J. Organomet. Chem.* **2015**, *791*, 183-191.
[11] C. Schmidt, B. Karge, R. Misgeld, A. Prokop, M. Brönstrup, I. Ott, *Med. Chem. Commun.* **2017**, *8*, 1681-1689.
[12] R. Rubbiani, S. Can, I. Kitanovic, H. Alborzinia, Maria Stefanopoulou, M. Kokoschka, S. Mönchgesang, W. S. Sheldrick, S. Wölfl, I. Ott, *J. Med. Chem.* **2011**, *54*, 8646-8657.
[13] A. Bindoli, M. P. Rigobello, G. Scutari, C. Gabbiani, A. Casini, L. Messori, *Coord. Chem. Rev.* **2009**, *253*, 1692-1707.
[14] R. Rubbiani, L. Salassa, A. de Almeida, A. Casini, I. Ott, *ChemMedChem* **2014**, *9*, 1205-1210.
[15] A. Citta, E. Schuh, F. Mohr, A. Folda, M. L. Massimino, A. Bindoli, A. Casini, M. P. Rigobello, *Metallomics* **2013**, *5*, 1006-1015.
[16] E. Schuh, C. Pflüger, A. Citta, A. Folda, M. P. Rigobello, A. Binhdoli, A. Casini, F. Mohr, *J. Med. Chem.* **2012**, *55*, 5518-5528.
[17] C. Schmidt, B. Karge, R. Misgeld, A. Prokop, R. Franke, M. Brönstrup, I. Ott, *Chem. Eur. J.* **2017**, *23*, 1869-1880.
[18] W. Liu, K. Bensdorf, M. Proetto, A. Hagenbach, U. Abram, R. Gust, *J. Med. Chem.* **2012**, *55*, 3713-3724.
[19] C. Bazzicalupi, M. Ferraroni, F. Papi, L. Massai, B. Bertrand, L. Messori, P. Gratteri, A. Casini, *Angew. Chem. Int. Ed.* **2016**, *55*, 4256-4259.
[20] J. K. Muenzner, B. Biersack, A. Albrecht, T. Rehm, U. Lacher, W. Milius, A. Casini, J.-J. Zhang, I. Ott, V. Brabec, O. Stuchlikova, I. C. Andronache, L. Kaps, D. Schuppan, R. Schobert, *Chem. Eur. J.* **2016**, *22*, 18953-18962.
[21] C. Zhang, S. Bourgeade Delmas, Á. Fernández Álvarez, A. Valentin, C. Hemmert, H. Gornitzka, *Eur. J. Med. Chem.* **2018**, 143, 1635-1643.
[22] C. Hemmert, A. Pramundita Ramadani, L. Boselli, A Fernández Álvarez, L. Paloque, J. M. Augereau, H. Gornitzka, F. Benoit-Vical, *Bioorg. Med. Chem.* **2016**, 24, 3075-3082.
[23] L. Boselli, M. Carraz, S. Mazères, L. Paloque, G. Gonzalez, F. Benoit-Vical, A. Valentin, C. Hemmert, H. Gornitzka, *Organometallics* **2015**, *34*, 1046-1055.
[24] L. Paloque, C. Hemmert, A. Valentin, H. Gornitzka, *Eur. J. Med. Chem.* **2015**, *94*, 22-29.
[25] L. Boselli, I. Ader, M. Carraz, C. Hemmert, O. Cuvillier, H. Gornitzka, *Eur. J. Med. Chem.* **2014**, *85*, 87-94.
[26] C. Hemmert, A. Fabié, A. Fabre, F. Benoit-Vical, H. Gornitzka, *Eur. J. Med. Chem.* **2013**, *60*, 64-75.
[27] T. Mosmann, *J. Immunol. Methods* **1983**, 65, 55-63.
[28] F. Rangwala, K. P.Williams, G. R. Smith, Z. Thomas, J. L. Allensworth, H. K. Lyerly, A. M. Diehl, M. A. Morse, G. R. Devi, *BMC Cancer* **2012**, *12*, 402.
[29] P. J. Barnard and S. J. Berners-Price, *Coord. Chem. Rev.* **2007**, *251*, 1889-1902.
[30] M. V. Baker, P. J. Barnard, S. J. Berners-Price, S. K. Brayshaw, J. L. Hickey, B. W. Skelton, A. H. White, *Dalton Trans.* **2006**, 3708-3715.
[31] J. L. Misset, H. Bleiberg, W. Sutherland, M. Bekradda, E. Cvitkovic, *Critical Reviews in Oncology:Hematology* **2000**, *35*, 75-93.
[32] W. P. McGuire, E. K. Rowinsky, N. B. Rosenhein, F. C. Grumbine, D. S. Ettinger, D. K. Armstrong, R. C. Donehower, *Ann. Intern. Med.* **1989**, *111*, 273-279.
[33] S. Ramalingam, C.P. Belani, *Expert Opin. Pharmacother*. **2004**, 5, 1771-1780.
[34] A. M. M. Yvon, P. Wadsworth, M. A. Jordan, *Mol. Biol. Cell* **1999**, *10,* 947-959.
[35] K. I. Fujita, Y. Kubota, H. Ishida, Y. Sasaki, *World J. Gastroenterol.* **2015**, *21,* 12234-12248.
[36] D. B. Longley, D. P. Harkin, P. G. Johnston, *Nat. Rev. Cancer* **2003**, *3*, 330-338.
[37] J. C. Hernandez-Boluda, F. Cervantes, *Drugs Today* **2002**, *38*, 601-613.
[38] J. M. Llovet, A. Burroughs, J. Bruix, *Lancet* **2003**, *362*, 1907-1917.
[39] R. Rubbiani, I. Kitanovic, H. Alborzinia, S. Can, A. Kitanovic, L. A. Onambele, M. Stefanopoulou, Y. Geldmacher, W. S. Sheldrick, G. Wolber, A. Prokop, S. Wölfl, I. Ott, *J. Med. Chem.* **2010**, *53*, 8608-8618.
[40] O. Rackham, S. J. Nichols, P. J. Leedman, S. J. Berners-Price, *Biochem. Pharmacol.* **2007**, *74*, 992-1002.
[41] J. L. Hickey, R. A. Ruhayel, P. J. Barnard, M. V. Baker, S. J. Berners-Price, *J. Am. Chem. Soc.* **2008**, *130*, 12570-12571.
[42] B. Bertrand, A. Casini, *Dalton Trans.* **2014**, *43*, 4209-4219.
[43] W. Liu, R. Gust, *Coord. Chem. Rev.* **2016**, *329*, 191-213.
[44] A. Holmgren, J. Lu, *Biochem. Biophys. Res. Commun.* **2010**, *396*, 120-124.

[45] S. J. Berners-Price, A. Filipovska, *Metallomics* **2011**, *3*, 863-873.
[46] A. Pratesi, C. Gabbiani, M. Ginanneschi, L Messori, *Chem. Commun.* **2010**, *46*, 7001-7003.
[47] C. Gabbiani, G. Mastrobuoni, F. Sorrentino, B. Dani, M. P. Rigobello, A. Bindoli, M. A Cinellu, G. Pieraccini, L. Messori, A. Casini, *Med. Chem. Commun.* **2011**, *2*, 50-54.
[48] J. F. Arambula, R. McCall, K. J. Sidoran, D. Magda, N. A. Mitchell, C. W. Bielawski, V. M. Lynch, J. L. Sessler, K. Arumugam, *Chem. Sci.* **2016**, *7*, 1245-1256.
[49] Y. Li, G. F. Liu, C .P. Tan, L .N. Ji, Z. W. Mao, *Metallomics* **2014**, *6*, 1460-1468.
[50] A. Nandy, S. K. Dey, S. Das, R. N. Munda, J. Dinda, K. D. Saha, *Mol. Cancer* **2014**, *13*, 57.
[51] B. D'Autréaux, M. B. Toledano, *Nat. Rev. Mol. Cell. Biol*. **2007**, *8*, 813–824.
[52] L. Tabrizi, H. Chiniforoshan, *Dalton Trans.* **2017**, *46*, 14164-14173.
[53] G. M. Sheldrick, *Acta Cryst*. **2008**, *A64*, 112–122.
[54] G. M. Sheldrick, *Acta Cryst.* **2015**, *C71*, 3-8.
[55] S. Parsons, H. D. Flack, T. Wagner, *Acta Cryst*. **2013**, *B69*, 249–259.
[56] Discovery Development Services | NCI-60 Human Cancer Cell Line Screen | List of Cell Lines https://dtp.cancer.gov/discovery_development/nci-60/methodology.htm.